Thermal cycling-hyperthermia ameliorates cognitive impairment of intracerebroventricular $A\beta_{25-35}$-induced Alzheimer's disease in C57BL/6 mice

Yu-Yi Kuo[1,2], Wei-Ting Chen[1,2], Guan-Bo Lin[1,2], You-Ming Chen[2,3], Hsu-Hsiang Liu[2,3], and Chih-Yu Chao[1,2,3,*]

[1] Department of Physics, Lab for Medical Physics & Biomedical Engineering, National Taiwan University, Taipei 10617, Taiwan

[2] Molecular Imaging Center, National Taiwan University College of Medicine, Taipei 10051, Taiwan

[3] Graduate Institute of Applied Physics, Biophysics Division, National Taiwan University, Taipei 10617, Taiwan

* Corresponding author

E-mail: cychao@phys.ntu.edu.tw (CYC)

Abstract

Despite continuation of some controversies, Alzheimer's disease (AD), the most common cause of dementia nowadays, has been widely believed to derive mainly from

excessive β-amyloid (Aβ) aggregation, that would increase reactive oxygen species (ROS) and induce neuroinflammation, leading to neuron loss and cognitive impairment. Existing drugs on Aβ have been ineffective or offer only temporary relief at best, due to blood-brain barrier or severe side effects. The study employed thermal cycling-hyperthermia (TC-HT) as an alternative AD therapy and compared its effect with continuous hyperthermia (HT) *in vivo*. It established an AD mice model via intracerebroventricular (i.c.v.) injection of $A\beta_{25-35}$, proving that TC-HT is much more effective in alleviating its performance decline in Y-maze and NOR test, in comparison with HT. In addition, TC-HT also exhibits a better performance in decreasing the hippocampal Aβ and BACE1 expressions as well as the neuroinflammation markers Iba-1 and GFAP levels. Furthermore, the study finds that TC-HT can elevate more protein expressions of IDE and antioxidative enzyme SOD2 than HT. Besides, after establishment of neuroprotective mechanism, removal of TC-HT-induced ROS can further augment protection of neural cells against Aβ. In sum, the study proves the potential of TC-HT in AD treatment, which can be put into clinical application with the use of high-intensity focused ultrasound (HIFU).

37 **Introduction**

38 Alzheimer's disease (AD) has been the most common cause of dementia
39 nowadays, accounting for over 60% of all the cases [1]. One of the most notable
40 hallmarks of AD pathogenesis is the accumulation in brain of toxic β-amyloid (Aβ)
41 peptides [2], which are cleaved from the amyloid precursor protein (APP) by β- and γ-
42 secretase [3]. Such abnormal Aβ deposits can activate neuroinflammation [4], generate
43 reactive oxygen species (ROS) [5, 6], and cause neuron dysfunction and synapse loss,
44 leading to memory loss and cognitive impairment [7, 8]. Therefore, Aβ appears to be
45 the foremost target in AD therapy [9].

46 Currently, drug therapy is the mainstream AD treatment, aiming to suppress the
47 generation [10], disrupt the aggregation [11], and promote the clearance [12] of Aβ.
48 Drugs on proteases, such as insulin degrading enzyme (IDE), for alleviating Aβ
49 degradation also have significant potential in AD treatment [13]. However, at present
50 AD drugs have high failure rates, due to difficulty penetrating blood-brain barrier, on
51 top of severe side effects, such as liver toxicity, strong autoimmune response, or
52 carcinogenicity [14]. Hence, there is a need for a safe and effective alternative AD
53 therapy.

54 Heat has long been regarded as an alternative therapy with significant potential,
55 given its proven therapeutic effect in physiotherapy, ophthalmology, and cardiology
56 [15]. Hyperthermia (HT), for instance, has been applied effectively in cancer treatment,
57 either for directly inhibiting tumor growth [16] or supplementing radiotherapy and
58 certain chemotherapies to augment their efficacy [17]. In addition, HT has also been
59 reported to be capable of increasing the expression of heat shock protein family [18],
60 some of whose members can suppress the formation of Aβ fibril and Aβ toxicity [19,
61 20]. Besides, HT treatment is conducive to increase the levels of IDE [21] and
62 antioxidant proteins, such as nuclear factor erythroid 2–related factor 2 (Nrf2) and
63 superoxide dismutase 2 (SOD2) [22, 23].

64 However, continuous high-temperature exposure can be thermotoxic to human
65 neural cells, according to some reports [24]. Heat stroke, featuring abnormally high
66 core body temperature (> 40°C), may cause cerebellar injury and memory deficits [25,
67 26]. Whole-body HT treatment has also been reported to cause adverse effect on
68 memory or neural system, such as decreased cognitive performance, impaired pressure-
69 flow autoregulation, brain edema, intracerebral hemorrhage, and transient central
70 nervous system dysfunction [27, 28]. Moreover, although a study showed that long-

71 term heat exposure could reduce the risk of memory loss among middle-aged men, it
72 was time-consuming without certain curative effect [29]. Therefore, it is imperative to
73 find a tolerable and effective thermal treatment for AD.

74 Our previous study put forth a novel thermal treatment, thermal-cycling
75 hyperthermia (TC-HT), demonstrating its therapeutic effect in anticancer treatment [30,
76 31] and neuroprotection [32] in vitro, with minimal side effects. The study applied TC-
77 HT to treat mice with AD, induced by intracerebroventricular (i.c.v.) injection of $A\beta_{25-}$
78 $_{35}$, for comparison with the therapeutic effect of HT. In both cases, heat was applied to
79 mouse brain specifically, to avoid potential side effect of whole-body HT.

80 In this paper, behavioral tests show that TC-HT significantly improves Aβ-
81 induced memory impairment, with an effect much better than HT. In addition, TC-HT
82 also exhibits a much better performance than HT in decreasing Aβ and β-secretase
83 (BACE1) expressions, suppressing neuroinflammation markers ionized calcium-
84 binding adapter molecule 1 (Iba-1) and glial fibrillary acidic protein (GFAP) levels,
85 and increasing the expression levels of IDE and SOD2 enzymes. Furthermore, the study
86 shows that removal of TC-HT-induced ROS can further augment the protective effect

87 of TC-HT in an in vitro neural model. In sum, these results underscore the potential of

88 TC-HT as an alternative AD therapy.

89

90 Materials and Methods

91 Ethics Statement

92 All animal experiments were conducted according to the regulations approved by

93 the Animal Ethical Committee of National Taiwan University. Mice were monitored

94 every day for signs of distress. The humane endpoints of the mice included decreased

95 socialization, anorexia, weight loss of 15%, hunching, or the inability to evade handling.

96 All hydrodynamic injections and thermal treatments were conducted under anesthesia

97 with 5% isoflurane (Panion & BF Biotech Inc., Taipei, Taiwan), and all efforts were

98 made to minimize suffering. For sacrifice, mice were humanely euthanized via carbon

99 dioxide (CO_2) gas asphyxiation followed by cervical dislocation and were considered

100 non-survivors.

101

102 Animals

103 C57BL/6 male mice (6-8 weeks old, 22-26 g) were obtained from National
104 Laboratory Animal Center (Taipei, Taiwan). All mice were housed in groups of 6 mice
105 per cage (32 cm × 16 cm × 14 cm) and maintained in a specific-pathogen-free (SPF)
106 room under controlled temperature (22±2 °C) and relative humidity (55±10%) in
107 Animal Resource Center of National Taiwan University. All mice were subjected to a
108 12:12 h light/dark cycle (lights on at 7:00 a.m.) with free access to food and water. All
109 experiments were conducted with mice at age 6-8 weeks. All mice were randomly
110 categorized into the control group, Aβ group, TC-HT group, and HT group.
111

112 **β-amyloid administration**

113 $A\beta_{25-35}$ (Sigma-Aldrich; Merck KGaA, Darmstadt, Germany) was dissolved in
114 0.9% sterile saline solution to a concentration of 1 mg/mL and then incubated at 37°C
115 for 7 days for fibril aggregation. At the beginning of the experiment (Day 0), 10 μL Aβ
116 solution was i.c.v.-injected into the mice's brains of the Aβ, TC-HT, and HT groups
117 [33]. 10 μL of sterile saline solution was i.c.v.-injected into the mice's brains of the
118 sham-operated control group
119

120 **HT and TC-HT treatments**

121 To focus on the thermal effect on mice's brain and minimize the potential
122 interference outside of brains by the conventional whole-body hyperthermia methods
123 [34-36], we adopted a modified method to heat mice's heads locally. As shown in **Fig**
124 **1A**, both HT and TC-HT thermal treatments were applied by a temperature controlling
125 and heating system equipped with a DC power supply (9303D, ABM Industries Inc.,
126 NY, USA), a temperature/process controller (PZ900, RKC instrument Inc., Tokyo,
127 Japan), and a 19 mm × 19 mm polyimide thermofoil for heating (HK5578R4.6L12A,
128 Minco Products Inc., Fridley, MN, USA). Mice were anesthetized with 5% isoflurane
129 during thermal treatments. Mice's head fur was shaved and the thermofoil was taped
130 onto the bare skin with a thin layer of vaseline for better attachment. The thermocouple
131 measuring tip (K-type) was located under the central region of the thermalfoil, as shown
132 in **Fig 1B**. The actual temperatures of mice's heads were measured via the K-type
133 thermocouple and monitored by the temperature/process controller. For TC-HT
134 treatment, the temperature/process controller was set to implement a 10-cycle repeated
135 procedure, in which each cycle is consisted of a desired high-temperature stage for a
136 period of time, followed by a natural thermal dissipating stage for 30 sec at low-

137 temperature setting 37 °C (**Fig 1C**). In the study, the high-temperature stage in TC-HT

138 treatment was held at 42 °C for 6 min with a 0.5 °C tolerance. For HT treatment, the

139 temperature was kept at 42 ± 0.5 °C continuously for 1 h. Monitored temperatures of

140 mice's heads by HT and TC-HT thermal treatments were shown in **Fig 1D**.

141

142 **Fig 1. Experimental setup and design of TC-HT.**

143 (A) The setup of the temperature controlling and heating system, containing a DC

144 power supply, a temperature/process controller, and a thermofoil for heating. (B) The

145 thermal treatment was locally performed on mice's heads by thermofoil, and their

146 temperatures were measured via a K-type thermocouple, whose measuring tip was

147 placed in the central circled region under the thermofoil. (C) Schematic diagram of the

148 TC-HT temperature-controlled programs with parameter settings, and (D) the

149 temperatures of mice's heads by HT and TC-HT thermal treatments were recorded

150 every 10 sec throughout the heating period.

151

152 **Experimental design**

153 At the beginning of the experiment (Day 0), 10 μL Aβ solution was i.c.v.-injected
154 into the mice's brains of the Aβ, TC-HT, and HT groups. On day 4, 8, and 12, the
155 respective thermal treatment was applied to the mice of the TC-HT and HT groups. Y-
156 maze and NOR tests were assessed on day 13 and day 14, respectively. Brain tissues
157 were collected after the Y-maze test for the following western blot analyses. The
158 experimental schedule was shown in **Fig 2**.
159
160 **Fig 2. The experimental schedule.**
161 Aβ solution was i.c.v.-injected at day 0, and the respective thermal treatment was
162 implemented at day 4, 8, and 12. Behavioral tests of NOR and Y-maze were carried out
163 at day 13 and 14, respectively. After the Y-maze test, mice were weighted and then
164 euthanized to collect brain tissues for the following western blot analyses.
165
166 **Y-maze test**
167 The Y-maze test was used to assess the spatial working memory of mice. The
168 apparatus is consisted of three identical arms (40 cm × 13 cm × 6.5 cm) interconnected
169 at a central junction at 120° each. The assessed mouse was placed at the end of the start

170 arm, and was allowed to explore all three arms freely for 8 min. The behavioral
171 performance was recorded, and the spontaneous index was calculated as follows:
172 (number of correct alternations) / (total number of arm entries – 2) × 100. In addition,
173 the total number of arm entries in the Y-maze was used as a measure to characterize
174 locomotor activity.
175

176 **Novel object recognition (NOR) test**

177 We used the NOR test to assess the recognition memory of animals. The NOR test
178 consists of a familiarization phase and a test phase. In the familiarization phase, the
179 assessed mouse was placed in a 40 cm × 40 cm × 30.5 cm box for 8 min with 2 identical
180 Lego blocks, which were placed close to two diagonal corners of the box. After the
181 familiarization phase, the mouse was returned to the home cage for 1 h and then was
182 placed back into the testing box for the test phase. One of the original objects was
183 replaced with a novel Lego block of a different shape in the test phase, and the
184 behavioral performance of the mouse was recorded with an overhead video camera for
185 8 min. Exploration was defined as sniffing or touching the object with the nose and/or
186 forepaws. The duration of the exploring time was calculated for the discrimination

187 index. A discrimination index was defined as follows: (Tn-To) / (Tn+To), where Tn
188 and To stand for the exploration time of the novel and original objects, respectively.
189

190 **Brain tissue collection and Western blot sample preparation**

191 Mice were euthanized by CO_2 gas. After confirming the death of mice, brains were
192 taken out quickly and rinsed with phosphate buffered saline (PBS) (HyClone; GE
193 Healthcare Life Sciences, Chicago, IL, USA) supplemented with 1% fresh protease
194 inhibitor cocktail (EMD Millipore, Billerica, MA, USA). Hippocampi were rapidly
195 dissected on an ice-cold plate, and then stored in ice-cold RIPA lysis buffer (EMD
196 Millipore) supplemented with 1% fresh protease inhibitor cocktail. Hippocampal
197 tissues were homogenized via ultrasound processing (5 sec rectangular pulse with 5 sec
198 interval for 3 times, amplitude 50%, by a Q125 sonicator; Qsonica, Newton, CT, USA)
199 and then centrifuged at 23000×g for 30 min at 4°C. The supernatants were collected
200 and the protein concentration was quantified by the Bradford protein assay (BioShop
201 Canada Inc., Burlington, Ontario, Canada). Protein samples were stored at -80°C for
202 subsequent western blotting assessments.
203

204 **Western blot analysis**

205 Proteins from the homogenized hippocampi were resolved by sodium dodecyl
206 sulfate polyacrylamide gel electrophoresis (SDS-PAGE) and then electroblotted onto
207 the polyvinylidene difluoride (PVDF) membranes (EMD Millipore). Blotted
208 membranes were blocked with 5% skim milk in Tris-buffered saline supplemented with
209 0.1% Tween-20 (TBST) (both from BioShop Canada Inc.) for 1 h at room temperature
210 (RT) and then incubated overnight with diluted primary antibodies in blocking buffer
211 at 4 °C, followed by three rinses with TBST washing buffer. Primary antibodies
212 employed in this study were listed as following: anti-Aβ (Santa Cruz Biotechnology,
213 Inc., Dallas, TX, USA), anti-IDE (Abcam, Cambridge, UK), anti-BACE1, anti-SOD2,
214 anti-Iba-1 (Cell Signaling Technology, Danvers, MA, USA), anti-GFAP, and anti-β-
215 actin (Gentex, Irvine, CA, USA). After washing with TBST, the membranes were
216 incubated with horseradish peroxidase-conjugated goat anti-mouse (for probing anti-
217 Aβ primary antibody) or goat anti-rabbit (for probing the other primary antibodies)
218 secondary antibodies (both from Jackson ImmunoResearch Laboratories, Inc., West
219 Grove, PA, USA) for 1 h at RT. All the antibodies were diluted according to the
220 manufacturer's instructions to their optimal concentration. The protein bands were

221 visualized by an enhanced chemiluminescence substrate (Advansta, San Jose, CA, USA)
222 and detected by an imaging system Amersham Imager 600 (GE Healthcare Life
223 Sciences). The images were analyzed with Image Lab software (Bio-Rad Laboratories,
224 Inc.). For normalization of proteins, β-actin was used as the loading control to
225 determine the relative folds of targeted proteins.
226

227 **In vitro cell culture and hydrogen gas (H_2) treatment**

228 The human neuroblastoma SH-SY5Y cells were purchased from American Type
229 Culture Collection (Manassas, VA, USA). The cell culture medium was MEM/F-12
230 mixture (HyClone; GE Healthcare Life Sciences) containing 10% fetal bovine serum
231 (HyClone; GE Healthcare Life Sciences) and 1% penicillin-streptomycin (Gibco Life
232 Technologies, Grand Island, NY, USA), supplemented with 1mM sodium pyruvate
233 (Sigma-Aldrich; Merck KGaA) and 0.1 mM non-essential amino acids (Invitrogen Life
234 Technologies, Grand Island, NY, USA). Cells were maintained in a humidified
235 incubator composed of 5% CO_2 at 37°C. Before the experiment, SH-SY5Y cells were
236 subcultured and seeded in 96-well plates (Thermo Fisher Scientific Inc., Waltham, MA,
237 USA) overnight. Cells were treated with 25 μM Aβ for 1 h and then subjected to the

238 TC-HT treatment for about 2 h. The TC-HT treatment was implemented by the Thermal
239 Cycler (Applied Biosystems; Thermo Fisher Scientific, Inc.) and the in vitro TC-HT
240 parameter settings were described in our previous study [32]. In the experiment, H_2-
241 mixed gas was composed of 75% H_2, 20% oxygen gas (O_2), and 5% CO_2 gas
242 (vol/vol/vol), as described elsewhere [37]. After continuous exposure to the H_2-mixed
243 gas, it has been observed that H_2 concentration of the culture medium in a closed acrylic
244 box gets saturated within 20~30 min at atmospheric pressure [38]. Upon 12~16 h after
245 TC-HT treatment, cultured SH-SY5Y cells were sent into an acrylic chamber of volume
246 about 450 mL. Mixed gas consisting of 75% H_2, 20% O_2, and 5% CO_2 (vol/vol/vol)
247 were well mixed and then flowed into the chamber at a rate of 400 mL/min for 90 min
248 under normal pressure. Upon 4 days after the Aβ administration, the 3-(4,5-
249 dimethylthiazol-2-yl)-2,5-diphenyltetrazolium bromide (MTT) (Sigma-Aldrich; Merck
250 KGaA) assay was used to analyze the cell viability of SH-SY5Y cells. In brief, the
251 culture medium was replaced with MTT solution (0.5 mg/mL in the MEM/F12 mixture)
252 and incubated at 37°C for 4 h. The formazan crystals were dissolved by equal volume
253 of the solubilizing buffer containing 10% sodium dodecyl sulfate (SDS) (Bioshop
254 Canada Inc.) solution in 0.01 N hydrochloric acid (HCl) (Echo Chemical Co. Ltd.,

255 Taiwan) at 37 °C overnight. The absorbance at 570 nm of each well was analyzed by
256 Multiskan GO microplate spectrophotometer (Thermo Fisher Scientific Inc.), and the
257 background absorbance at 690 nm was subtracted. The cell viability of each group was
258 expressed as percentage of the untreated control.
259

260 **Statistical Analysis**

261 All statistical results were shown as mean ± standard deviation (S.D.). Statistical
262 analysis was conducted with OriginPro 2015 software (OriginLab Corporation,
263 Northampton, MA, USA) using one-way analysis of variance (ANOVA), followed by
264 Tukey's post hoc test. P-value < 0.05 was considered to indicate a statistically
265 significant difference.
266

267 ## Results

268 **TC-HT improves Aβ-induced recognition impairments in mice**

269 The study employed Y-maze test and NOR test to examine the therapeutic effect
270 of TC-HT and HT on AD mice. In the Y-maze test, the overall percentage of each

271 mouse's spontaneous index was computed to show its short-term memory function. As
272 exhibited in **Fig 3A**, the spontaneous index of the Aβ group is inhibited significantly,
273 ranging from 60.3% to 44.1%, compared with the control group. TC-HT significantly
274 improves the memory deficiency, elevating the spontaneous index to 61.6%, notably
275 different from HT, which only causes an insignificant improvement (spontaneous index
276 46.8%). Besides, there is no significant difference in the total number of arm entries
277 among the four groups (**Fig 3B**), suggesting that i.c.v. Aβ injection or both thermal
278 treatments didn't affect the locomotor activities of mice. On the other hand, NOR test
279 also confirmed that TC-HT is more effective in alleviating Aβ-induced memory
280 impairment than HT. As shown in **Fig 3C**, along with memory decline, the
281 discrimination index of the Aβ group plunged from 25.1% down to -26.2%, which
282 bounces back to 19.2% after TC-HT treatment, significantly outperforming HT
283 treatment, which only raises the discrimination index to -3.1%. Thus, TC-HT exhibited
284 a much stronger reversing effect on cognitive impairment than HT in both Y-maze and
285 NOR tests.
286
287 **Fig 3. Effect of TC-HT and HT treatments on mice's behavioral performances.**

288 The recovery effects of Aβ-induced recognition impairments after TC-HT and HT
289 treatments are assessed via (A) the spontaneous index and (B) the total number of arm
290 entries in the Y-maze test, and (C) the discrimination index in the NOR test. Data are
291 presented as mean ± S.D. (n = 9 in each group). One-way ANOVA with Tukey's post
292 hoc test is used to determine statistical significance (*P < 0.05 between indicated
293 groups).
294

295 **TC-HT down-regulates Aβ secretion and accumulation in mouse brain**

296 The study first analyzed the accumulated Aβ levels in hippocampi, confirming the
297 significant effect of TC-HT treatment in repairing Aβ-induced cognitive impairment,
298 as it reduces the hippocampal Aβ level from 1.34-fold to 0.88-fold compared to the
299 control group (**Fig 4A**). HT treatment, by comparison, exhibited only slight inhibitive
300 effect on the hippocampal Aβ level (1.24-fold). On the other hand, it is realized that Aβ
301 level in mouse brain is partially attributed to the pathological changes of BACE1 [39].
302 In **Fig 4B**, our results show that i.c.v.-injected Aβ triggers a significant increase in
303 hippocampal BACE1 expression (1.30-fold) compared with the control group. The
304 study finds that the elevation of BACE1 expression is significantly suppressed by the

305 TC-HT treatment (0.89-fold), but only slightly decreased by the HT treatment (1.19-
306 fold). It's noteworthy that there is no significant difference in BACE1 levels between
307 the Aβ group and the HT group, suggesting that conventional HT treatment is
308 ineffective in stopping abnormal Aβ secretion in mouse brain. To the best of our
309 knowledge, this is the first time that a thermal treatment exhibited an inhibitory ability
310 on the expression level of BACE1. In sum, the study shows that TC-HT appears to be
311 much more effective AD treatment than HT, as it's more capable of regulating Aβ
312 levels actively and inhibiting BACE1 level in hippocampus.
313
314 **Fig 4. Effect of TC-HT and HT treatments on the expression levels of Aβ and**
315 **BACE1 in hippocampi.**
316 Representative western blots and the quantifications of (A) Aβ and (B) BACE1 are
317 presented for evaluating anti-Aβ effect in hippocampi. β-actin was used as loading
318 control. Data are presented as mean ± S.D. (n = 9 in each group). One-way ANOVA
319 with Tukey's post hoc test is used to determine statistical significance (*$P < 0.05$
320 between indicated groups).
321

322 **TC-HT ameliorates Aβ-induced neuroinflammation in mouse brain**

323 Neuroinflammation is another hallmark of AD, as the risk of cognitive impairment
324 is highly associated with inflammatory level [40]. The study finds that the expression
325 levels of both hippocampal Iba-1 and GFAP, the activation markers of microglia cells
326 and astrocytes, respectively, are significantly enhanced in the Aβ group, compared with
327 the control group (**Fig 5A** and **5B**). After the TC-HT treatment, both Iba-1 and GFAP
328 levels drop significantly, while the HT treatment only slightly attenuates their
329 expression levels. There is no significant difference between the Aβ group and the HT
330 group in the expressions of both Iba-1 and GFAP. The results indicate that TC-HT
331 treatment can better ameliorate Aβ-induced neuroinflammation than HT treatment *in*
332 *vivo*.

333

334 **Fig 5. Effect of TC-HT and HT treatments on the expression levels of**
335 **neuroinflammatory markers Iba-1 and GFAP in hippocampi.**
336 Representative western blots and the quantifications of (A) Iba-1 and (B) GFAP are
337 presented for evaluating anti-neuroinflammation effect in hippocampi. β-actin was used
338 as loading control. Data are presented as mean ± S.D. (n = 9 in each group). One-way

339 ANOVA with Tukey's post hoc test is used to determine statistical significance (*P <

340 0.05 between indicated groups).

341

342 **TC-HT promotes the expressions of IDE and SOD2 proteins in mouse brain**

343 With IDE long regarded as a major endogenous enzyme attributing to Aβ

344 degradation, the alteration of IDE activity and expression can cause Aβ accumulation,

345 thereby increasing the risk of AD [41]. **Fig 6A** shows that while Aβ injection slightly

346 decreases the hippocampal IDE level (0.88-fold), TC-HT treatment significantly

347 increases the IDE expression level in hippocampi up to 1.38-fold. By contrast, HT

348 treatment performs an insignificant altering effect on IDE expression (0.91-fold),

349 compared with the Aβ group. The findings show that TC-HT can intensify Aβ clearance

350 via elevating the IDE expression level in hippocampi, while HT is ineffective in

351 promoting the hippocampal IDE level and thus cannot contribute to the removal of

352 abnormal hippocampal Aβ in mice.

353 Antioxidant protein SOD2 also has significant potential in AD treatment, capable

354 of decreasing hippocampal superoxide and amyloid plaque in AD mice [42]. **Fig 6B**

355 shows that after i.c.v. Aβ injection, the SOD2 expression level drops significantly

356 (0.62-fold), which, though, recovers significantly in the TC-HT group (1.41-fold),
357 much higher than recovery to 0.86-fold after HT treatment. The results show that TC-
358 HT can activate stronger antioxidant activity in hippocampus against the Aβ-induced
359 oxidative stress than continuous HT *in vivo*.
360
361 **Fig 6. Effect of TC-HT and HT treatments on the expression levels of**
362 **neuroprotective proteins IDE and SOD2 in hippocampi.**
363 Representative western blots and the quantifications of (A) IDE and (B) SOD2 are
364 presented for evaluating Aβ clearance and antioxidant effect in hippocampi,
365 respectively. β-actin was used as loading control. Data are presented as mean ± S.D. (n
366 = 9 in each group). One-way ANOVA with Tukey's post hoc test is used to determine
367 statistical significance (*$P < 0.05$ between indicated groups).
368
369 **H_2 treatment produces auxiliary neuroprotective effect against Aβ after TC-HT**
370 **treatment in vitro**
371 To examine whether removal of excessive ROS after TC-HT treatment can
372 intensify the neuroprotective effect against Aβ, H_2 treatment as mentioned in Materials

373 and Methods section was introduced as an exogenous ROS scavenger in an in vitro
374 model. **Fig 7A** shows the significant suppression of the viability of SH-SY5Y cells to
375 60.9% under the insult of 25 μM Aβ, which recovers greatly to 82.5% after TC-HT
376 treatment. Moreover, we find that with a 90 min H_2 treatment at 12~16 h after TC-HT
377 treatment, the cell viability can bounce back to a near-normal level (96.0%), exhibiting
378 a better neuroprotective effect than TC-HT treatment alone. However, it should be
379 noted that administration of H_2 treatment less than 12 h after TC-HT treatment fails to
380 further boost the viability of SH-SY5Y cells. On the other hand, H_2 treatment alone
381 does not show any significant protective effect on SH-SY5Y cells against Aβ (**Fig 7B**).
382 These findings show that while removal of ROS via H_2 treatment alone has no effect
383 against Aβ, it can further enhance the neuroprotective effect of TC-HT treatment
384 against Aβ, exhibiting a better neuroprotective effect than TC-HT treatment alone. This
385 could be attributed to removal of TC-HT-induced ROS with H_2 treatment after
386 establishment of neuroprotective mechanism at 12~16 h after TC-HT treatment. These
387 results shed light on the approach in developing AD treatment.
388

389 **Fig 7. H_2 treatment as a ROS scavenger helps to promote further the**

390 **neuroprotective effect of TC-HT against Aβ in vitro.**

391 (A) Cell viabilities of SH-SY5Y cells treated with Aβ, Aβ + TC-HT, and Aβ + TC-HT

392 + H_2 treatment, respectively. The data show that H_2-assisted TC-HT treatment exhibits

393 a better neuroprotective effect than TC-HT treatment alone. In the other experiment,

394 SH-SY5Y cells were subjected directly to H_2 treatment after the administration of 25

395 μM Aβ. Cell viabilities of SH-SY5Y cells treated with Aβ and Aβ + H_2 treatment alone

396 are respectively shown in (B). The result indicates that H_2 treatment alone has no effect

397 against Aβ. Data are presented as mean ± S.D. (n = 6 in each group). One-way ANOVA

398 with Tukey's post hoc test is used to determine statistical significance (*$P < 0.05$

399 between indicated groups).

400

401 ## Discussion

402 Given prevalence of AD in our society in recent years, many scientists have taken

403 part in research on its treatment with various approaches, including Aβ hypothesis, one

404 of the most noticeable pathogenesis of AD [43]. Aβ peptides could be secreted in brains,

405 but their abnormal depositions, especially in hippocampus, could induce severe

406 neurodegeneration and synapse loss, thereby impairing memory and cognitive abilities
407 [7, 8]. The study employed $A\beta_{25-35}$, peptide fragment of $A\beta_{1-42}$ considered the most
408 pathogenic Aβ species in AD [44, 45], as the model. Development of AD drugs has
409 been confronted with two major obstacles, namely blood-brain barrier (BBB) and
410 severe side effects [14, 46]. Hence, the application of heat has potential as an alternative
411 AD treatment, due to its capability to intensify neuroprotective effect [32] and sidestep
412 BBB, targeting the diseased brain directly. The study embraced TC-HT, a modified
413 heat treatment with higher safety and superior protective effect than HT [32], to
414 investigate the therapeutic potential of thermal treatment on AD *in vivo*.

415 With memory loss being the first and main symptom of AD [47], AD studies with
416 mice as model have often employed Y-maze and NOR tests to assess short-term
417 memory and learning memory [48, 49]. The study probed the therapeutic effect of HT
418 and TC-HT treatment on Aβ-induced memory impairment, finding that TC-HT
419 treatment can significantly improve the performance of spontaneous index (**Fig 3A**)
420 and help memory-impaired mice recognize and remember new objects (**Fig 3C**). The
421 study demonstrates significant effect of TC-HT treatment in recovering spatial working
422 memory and recognition memory impaired by Aβ. In comparison, although HT

423 treatment also enhances behavioral performance, the extent of improvement
424 significantly lags behind that of TC-HT treatment in both tests. Collectively, TC-HT
425 treatment exhibits a higher therapeutic potential than HT treatment in improving Aβ-
426 induced memory deficiency and cognitive dysfunction *in vivo*.

427 From a molecular perspective, Aβ hypothesis has long been a mainstream
428 approach in the study on the mechanism of AD pathogenesis and drug development
429 [50]. Under normal conditions, α- and γ-secretase will hydrolyze APP, preventing
430 production of Aβ peptides. However, once pathological changes occur, the hydrolysis
431 of APP is carried out by β- and γ-secretase, leading to secretion of toxic Aβ peptides
432 and aggregation of insoluble Aβ fibrils [3]. Thus, under the Aβ hypothesis, inhibition
433 of BACE1 is also considered a major therapeutic target, on top of Aβ clearance, in AD
434 treatment. The study exhibits the significant effect of TC-HT in decreasing the
435 hippocampal Aβ level, remarkably outperforming HT which fails to show any
436 significant Aβ clearance ability (**Fig 4A**). Besides, TC-HT also shows a significantly
437 better effect in inhibiting the hippocampal BACE1 level than HT, and there is no
438 significant difference in BACE1 level between the HT and Aβ groups (**Fig 4B**). These
439 results demonstrate that TC-HT can attenuate the amount of toxic Aβ fragments and

440 their production in the brains of AD mice, much better than the continuous HT
441 treatment. To the best of our knowledge, this is the first time that a physical thermal
442 treatment is proven to be able to modulate the expression of BACE1, shedding light on
443 alternative approach in AD treatment.

444 Apart from neurotoxic Aβ in brain, the pathogenesis of AD is also closely linked
445 to the activation of the brain's immune cells, particularly microglia and astrocytes,
446 which are triggered by Aβ deposits, according to some reports [4, 51]. Chronic
447 activation of the immune cells causes neuroinflammation, releasing the inflammatory
448 mediators which are associated with neurodegeneration and thus exacerbating AD
449 progression [51, 52]. Consequently, inhibition of neuroinflammation in AD brains is
450 also important in AD treatment. The study demonstrates extraordinary anti-
451 neuroinflammatory ability of TC-HT treatment. It is capable of suppressing both Aβ-
452 induced activation markers of microglial cells (Iba-1) and astrocytes (GFAP)
453 significantly, as shown in **Fig 5**. By contrast, the continuous HT treatment shows only
454 little inhibition on both neuroinflammatory markers without significance. Therefore,
455 the study proves that TC-HT is more capable of ameliorating neuroinflammation in AD
456 brains than continuous HT *in vivo*.

457 The clearance of toxic Aβ deposits, a hallmark of Alzheimer's disease, is as
458 important as curbing its production. First discovered as an enzyme responsible for the
459 degradation of insulin, IDE has also been found in recent studies to be capable of
460 degrading several polypeptides including Aβ [41]. In addition, it has been known that
461 neuron cells are able to regulate the extracellular levels of Aβ via proteolysis by IDE in
462 vitro [53]. Studies have also shown that the alteration of IDE plays a key role in AD,
463 as the decrease of IDE activity and expression could result in Aβ accumulation, thereby
464 raising the risk of AD development [54, 55]. In line with the finding of a recent study
465 that IDE can be increased in a fashion like heat shock protein (HSP) [21], our study
466 discovers that TC-HT treatment can significantly boost the hippocampal IDE level (**Fig**
467 **6A**), an effect unfound in HT treatment. The more pronounced Aβ clearance effect of
468 TC-HT may result from its higher capability in inhibiting Aβ production (**Fig 4B**) and
469 clearing Aβ (**Fig 6A**) than continuous HT, indicating its higher potential in AD therapy
470 than the latter.

471 Antioxidant enzyme is also an important protective mechanism against AD. It has
472 been known that Aβ deposition in brain can increase the production of mitochondrial
473 ROS and intracellular oxidative stress, increasing Aβ formation, which leads to a

474 vicious cycle and exacerbates AD progression [5, 6]. Besides, excessive ROS level
475 could be toxic to brain neurons and decrease cognitive performance, according to some
476 studies [56]. SOD2, a member of the superoxide dismutase family, can transform
477 superoxide $O_2^{\cdot -}$ into hydrogen peroxide and hence regulate excessive oxidative stress
478 [57]. The reduction of SOD2 can accelerate the onset of Aβ-dependent memory deficits
479 *in vivo* [58], while the elevation of SOD2 can prevent the memory deficits [59]. Our
480 study shows that TC-HT can greatly recover hippocampal SOD2 decreased by Aβ (**Fig**
481 **6B**), at a scale far outpacing that of HT. The result is in line with the behavioral
482 performance of mice in Y-maze and NOR tests in **Fig 3**, indicating that TC-HT can
483 attenuate the Aβ-induced memory deficits via removal of excessive ROS in brains by
484 SOD2-related mechanisms.

485 Excessive ROS accumulation could be detrimental to neurons, damaging memory
486 and cognitive ability. However, some studies have shown that proper increase of ROS
487 level is essential for activating the redox signalling and the associated neuroprotective
488 pathways [60]. Therefore, the study suggests not to eliminate ROS induced by thermal
489 stress, until setup of relevant protective mechanisms. To validate the hypothesis, an in
490 vitro experiment using H_2 treatment as an ROS scavenger was introduced in this study.

491 As shown in **Fig 7A**, the result shows significant recovery of the Aβ-inhibited viability
492 of SH-SY5Y cells after TC-HT treatment, whose neuroprotective effect could be
493 attributed to activation of Akt and its downstream signalling pathways, as suggested in
494 our previous study [32]. It has been reported that early administration of antioxidants
495 may block the construction of neuroprotection via these pathways [61-63], which is in
496 line with the observation that administration of H_2 treatment less than 12 h after TC-
497 HT fails to further augment the viability of SH-SY5Y cells. On the other hand, our
498 study shows that with 90 min H_2 treatment at 12~16 h after TC-HT, removal of TC-
499 HT-induced ROS can further boost protection of neural cells against Aβ, exhibiting a
500 better neuroprotective effect than TC-HT treatment alone (**Fig 7A**). Noticeably, the H_2
501 treatment alone did not show any protective effect for SH-SY5Y cells against 25 μM
502 Aβ (**Fig 7B**), indicating that TC-HT treatment is essential for the protective mechanism.
503 The results show that scavenging TC-HT-induced ROS with H_2 treatment after
504 establishment of neuroprotective mechanism by TC-HT (12~16 h after TC-HT
505 treatment) can further enhance the neuroprotective effect of TC-HT treatment against
506 Aβ. Relevant studies have been in progress *in vivo*.

507 In addition to the inhibitive effect of ROS on viability, continuous heat exposure
508 may hinder the function of neuroprotective proteins. Some studies have shown that the
509 inactivation of proteins may start around 40°C, due to protein denaturation and
510 unfolding [64]. In the study, continuous HT treatment doesn't exhibit significant effect
511 in Aβ regulation (**Fig 4 & Fig 6A**) and anti-neuroinflammation activity (**Fig 5**), and
512 lags behind TC-HT treatment in antioxidative activity (**Fig 6B**). However, with
513 identical heat exposure time, TC-HT featuring intermittent high-temperature treatment
514 attains much greater improvement than continuous HT. As a result, despite its
515 contribution to brain's neuroprotective mechanism, HT treatment may entail
516 overheating causing protein dysfunction in neural cells and thus interrupting the
517 pathways for neuroprotection. Therefore, the interspersing low-temperature process is
518 crucial for TC-HT treatment's neuroprotective effect. Our study demonstrates that TC-
519 HT can be an effective thermal treatment for AD. In practice, high-intensity focused
520 ultrasound (HIFU) may be a suitable heating source for TC-HT treatment, as it is
521 capable of precisely modulating the temperature at the targeted area, via computer-
522 controlled programmable procedure. The HIFU heating area can be set at only about 4-
523 8 mm [65, 66], smaller than human brain, thereby quickening heat dissipation to

524 surrounding tissues and preventing hyperthermic damage. In operation, multi-focal
525 HIFU can control the heating area and temperature by tuning the size of scanned spot
526 and intensity in scanning mode, thereby attaining set temperature and effective thermal
527 dissipation for TC-HT in AD treatment.

528 In summary, our study puts forth a novel hyperthermic method, TC-HT, for
529 application as a potential AD treatment *in vivo*, which demonstrates a better effect in
530 improving the cognitive performance of mice in Y-maze and NOR tests than
531 conventional HT treatment, which heats the subjects continuously. Furthermore, the
532 study shows that TC-HT can suppress the hippocampal Aβ expression to a normal level,
533 significantly outperforming HT which only exhibits a slight inhibition effect, perhaps
534 due to TC-HT's higher capability in inhibiting the Aβ productive activity of BACE1
535 protein and promoting the Aβ clearance effect of IDE protein. In addition, TC-HT can
536 significantly inhibit the Aβ-induced overexpression of neuroinflammatory markers Iba-
537 1 and GFAP in hippocampi, while HT treatment only slightly attenuates their
538 expression levels without significance. Moreover, TC-HT raises the expression level of
539 antioxidative protein SOD2 at an extent much higher than HT, indicating that it can
540 provide a better protection for hippocampal neurons against the i.c.v.-injected Aβ.

Overall, the study validates the therapeutic potential of TC-HT for AD *in vivo*, shedding light on development of alternative AD treatment with high efficacy.

Funding

This work was supported by grants from Ministry of Science and Technology (MOST 110-2112-M-002-004, MOST 109-2112-M-002-004, and MOST 108-2112-M-002-016 to CYC) of the Republic of China. The funders had no role in study design, data collection and analysis, decision to publish, or preparation of the manuscript.

Competing Interests

The authors have declared that no competing interests exist.

Acknowledgments

The authors would like to acknowledge the service provided by Animal Resource Center of National Taiwan University for facility support.

Author Contributions

Conceptualization: Chih-Yu Chao.

Data Curation: Yu-Yi Kuo, Chih-Yu Chao.

Formal analysis: Yu-Yi Kuo, Wei-Ting Chen, Guan-Bo Lin, You-Ming Chen, Hsu-Hsiang Liu, Chih-Yu Chao.

Funding acquisition: Chih-Yu Chao.

Investigation: Yu-Yi Kuo, Wei-Ting Chen, Guan-Bo Lin, Chih-Yu Chao.

Project Administration: Chih-Yu Chao.

Supervision: Chih-Yu Chao.

Validation: Yu-Yi Kuo, Wei-Ting Chen, Guan-Bo Lin, You-Ming Chen, Hsu-Hsiang Liu

Writing – original draft: Yu-Yi Kuo, Chih-Yu Chao.

Writing – review & editing: Chih-Yu Chao.

References

1. 2020 Alzheimer's disease facts and figures. Alzheimer's Dement. 2020; 16(3):391-460.
2. Chen GF, Xu TH, Yan Y, Zhou YR, Jiang Y, Melcher K, et al. Amyloid beta: structure, biology and structure-based therapeutic development. Acta Pharmacol Sin. 2017; 38(9):1205-35.

578 3. Sun X, Chen WD, Wang YD. β-amyloid: the key peptide in the pathogenesis of
579 Alzheimer's disease. Front Pharmacol. 2015; 6:221.
580 4. Essa MM, Subash S, Akbar M, Al-Adawi S, Guillemin GJ. Long-term dietary
581 supplementation of pomegranates, figs and dates alleviate neuroinflammation
582 in a transgenic mouse model of Alzheimer's disease. PLoS One. 2015;
583 10(3):e0120964.
584 5. García-Escudero V, Martín-Maestro P, Perry G, Avila J. Deconstructing
585 mitochondrial dysfunction in Alzheimer disease. Oxid Med Cell Longev. 2013;
586 2013:162152.
587 6. Leuner K, Schütt T, Kurz C, Eckert SH, Schiller C, Occhipinti A, et al.
588 Mitochondrion-derived reactive oxygen species lead to enhanced amyloid beta
589 formation. Antioxid Redox Signal. 2012; 16(12):1421-33.
590 7. Palop JJ, Mucke L. Amyloid-β-induced neuronal dysfunction in Alzheimer's
591 disease: from synapses toward neural networks. Nat Neurosci. 2010; 13(7):812-
592 8.
593 8. Kashyap G, Bapat D, Das D, Gowaikar R, Amritkar RE, Rangarajan G, et al.
594 Synapse loss and progress of Alzheimer's disease - a network model. Sci Rep.
595 2019; 9(1):6555.
596 9. Karran E, Mercken M, De Strooper B. The amyloid cascade hypothesis for
597 Alzheimer's disease: an appraisal for the development of therapeutics. Nat Rev
598 Drug Discov. 2011; 10(9):698-712.
599 10. Cao J, Hou J, Ping J, Cai D. Advances in developing novel therapeutic strategies
600 for Alzheimer's disease. Mol Neurodegener. 2018; 13(1):64.
601 11. Du Z, Li M, Ren J, Qu X. Current strategies for modulating Aβ aggregation
602 with multifunctional agents. Acc Chem Res. 2021; 54(9):2172-84.
603 12. Lee D, Lee G, Yoon DS. Anti-Aβ drug candidates in clinical trials and
604 plasmonic nanoparticle-based drug-screen for Alzheimer's disease. Analyst.
605 2018; 143(10):2204-12.
606 13. Xin SH, Tan L, Cao X, Yu JT, Tan L. Clearance of amyloid beta and tau in
607 Alzheimer's disease: from mechanisms to therapy. Neurotox Res. 2018;
608 34(3):733-48.
609 14. Hung SY, Fu WM. Drug candidates in clinical trials for Alzheimer's disease. J
610 Biomed Sci. 2017; 24(1):47.
611 15. Habash RW, Bansal R, Krewski D, Alhafid HT. Thermal therapy, part 1: an
612 introduction to thermal therapy. Crit Rev Biomed Eng. 2006; 34(6):459-89.

613 16. Manning MR, Cetas TC, Miller RC, Oleson JR, Connor WG, Gerner EW.
614 Clinical hyperthermia: results of a phase I trial employing hyperthermia alone
615 or in combination with external beam or interstitial radiotherapy. Cancer. 1982;
616 49(2):205-16.
617 17. Falk MH, Issels RD. Hyperthermia in oncology. Int J Hyperthermia. 2001;
618 17(1):1-18.
619 18. Tabuchi Y, Kondo T. Targeting heat shock transcription factor 1 for novel
620 hyperthermia therapy (review). Int J Mol Med. 2013; 32(1):3-8.
621 19. Rivera I, Capone R, Cauvi DM, Arispe N, De Maio A. Modulation of
622 Alzheimer's amyloid β peptide oligomerization and toxicity by extracellular
623 Hsp70. Cell Stress Chaperones. 2018; 23(2):269-79.
624 20. Wilhelmus MM, Boelens WC, Otte-Höller I, Kamps B, de Waal RM, Verbeek
625 MM. Small heat shock proteins inhibit amyloid-β protein aggregation and
626 cerebrovascular amyloid-β protein toxicity. Brain Res. 2006; 1089(1):67-78.
627 21. Tundo GR, Sbardella D, Ciaccio C, Bianculli A, Orlandi A, Desimio MG, et al.
628 Insulin-degrading enzyme (IDE): a novel heat shock-like protein. J Biol Chem.
629 2013; 288(4):2281-9.
630 22. Ahmed K, Zaidi SF, Mati-Ur-Rehman, Rehman R, Kondo T. Hyperthermia and
631 protein homeostasis: cytoprotection and cell death. J Therm Biol. 2020;
632 91:102615.
633 23. Banerjee Mustafi S, Chakraborty PK, Dey RS, Raha S. Heat stress upregulates
634 chaperone heat shock protein 70 and antioxidant manganese superoxide
635 dismutase through reactive oxygen species (ROS), p38MAPK, and Akt. Cell
636 Stress Chaperones. 2009; 14(6):579-89.
637 24. Hashemi M, Abbasiazam A, Oraee-Yazdani S, Lenzer J. Response of human
638 glioblastoma cells to hyperthermia: cellular apoptosis and molecular events.
639 Tissue Cell. 2022; 75:101751.
640 25. McLaughlin CT, Kane AG, Auber AE. MR imaging of heat stroke: external
641 capsule and thalamic T1 shortening and cerebellar injury. AJNR Am J
642 Neuroradiol. 2003; 24(7):1372-5.
643 26. Lee JS, Choi JC, Kang SY, Kang JH, Park JK. Heat stroke: increased signal
644 intensity in the bilateral cerebellar dentate nuclei and splenium on diffusion-
645 weighted MR imaging. AJNR Am J Neuroradiol. 2009; 30(4):e58.
646 27. Walter EJ, Carraretto M. The neurological and cognitive consequences of
647 hyperthermia. Crit Care. 2016; 20(1):199.

648 28. Cremer OL, Diephuis JC, van Soest H, Vaessen PH, Bruens MG, Hennis PJ, et
649 al. Cerebral oxygen extraction and autoregulation during extracorporeal whole
650 body hyperthermia in humans. Anesthesiology. 2004; 100(5):1101-7.
651 29. Laukkanen T, Kunutsor S, Kauhanen J, Laukkanen JA. Sauna bathing is
652 inversely associated with dementia and Alzheimer's disease in middle-aged
653 Finnish men. Age Ageing. 2017; 46(2):245-9.
654 30. Lu CH, Chen WT, Hsieh CH, Kuo YY, Chao CY. Thermal cycling-
655 hyperthermia in combination with polyphenols, epigallocatechin gallate and
656 chlorogenic acid, exerts synergistic anticancer effect against human pancreatic
657 cancer PANC-1 cells. PLoS One. 2019; 14(5):e0217676.
658 31. Chen WT, Sun YK, Lu CH, Chao CY. Thermal cycling as a novel thermal
659 therapy to synergistically enhance the anticancer effect of propolis on PANC-1
660 cells. Int J Oncol. 2019; 55(3):617-28.
661 32. Chen WT, Kuo YY, Lin GB, Lu CH, Hsu HP, Sun YK, et al. Thermal cycling
662 protects SH-SY5Y cells against hydrogen peroxide and β-amyloid-induced cell
663 injury through stress response mechanisms involving Akt pathway. PLoS One.
664 2020; 15(10):e0240022.
665 33. Kim HY, Lee DK, Chung BR, Kim HV, Kim Y. Intracerebroventricular
666 injection of amyloid-β peptides in normal mice to acutely induce Alzheimer-
667 like cognitive deficits. J Vis Exp. 2016; (109):53308.
668 34. Al Faruque H, Choi ES, Lee HR, Kim JH, Park S, Kim E. Targeted removal of
669 leukemia cells from the circulating system by whole-body magnetic
670 hyperthermia in mice. Nanoscale. 2020; 12(4):2773-86.
671 35. Lin C, Liu Z, Li Y, Chen J. Protocol for fever-range whole-body hyperthermia
672 (WBH) in mice to study febrile effect on T-cell adhesion and migration. STAR
673 Protoc. 2021; 2(3):100720.
674 36. Saim H, Salim MIM, Jemon K. Antitumor effect of fever range whole body
675 hyperthermia with curcumin in breast cancer-induced mice. Int J Recent
676 Technol Eng. 2019; 8(2):297-301.
677 37. Ohsawa I, Ishikawa M, Takahashi K, Watanabe M, Nishimaki K, Yamagata K,
678 et al. Hydrogen acts as a therapeutic antioxidant by selectively reducing
679 cytotoxic oxygen radicals. Nat Med. 2007; 13(6):688-94.
680 38. Murakami Y, Ito M, Ohsawa I. Molecular hydrogen protects against oxidative
681 stress-induced SH-SY5Y neuroblastoma cell death through the process of
682 mitohormesis. PLoS One. 2017; 12(5):e0176992.

683 39. Hampel H, Vassar R, De Strooper B, Hardy J, Willem M, Singh N, et al. The
684 β-secretase BACE1 in Alzheimer's disease. Biol Psychiatry. 2021; 89(8):745-
685 56.
686 40. Huang W, Li Z, Zhao L, Zhao W. Simvastatin ameliorate memory deficits and
687 inflammation in clinical and mouse model of Alzheimer's disease via
688 modulating the expression of miR-106b. Biomed Pharmacother. 2017; 92:46-
689 57.
690 41. Tundo GR, Sbardella D, Ciaccio C, Grasso G, Gioia M, Coletta A, et al.
691 Multiple functions of insulin-degrading enzyme: a metabolic crosslight? Crit
692 Rev Biochem Mol Biol. 2017; 52(5):554-82.
693 42. Massaad CA, Washington TM, Pautler RG, Klann E. Overexpression of SOD-
694 2 reduces hippocampal superoxide and prevents memory deficits in a mouse
695 model of Alzheimer's disease. Proc Natl Acad Sci USA. 2009; 106(32):13576-
696 81.
697 43. Selkoe DJ, Hardy J. The amyloid hypothesis of Alzheimer’s disease at 25 years.
698 EMBO Mol Med. 2016; 8(6):595-608.
699 44. Naldi M, Fiori J, Pistolozzi M, Drake AF, Bertucci C, Wu R, et al. Amyloid β-
700 peptide 25-35 self-assembly and its inhibition: a model undecapeptide system
701 to gain atomistic and secondary structure details of the Alzheimer’s disease
702 process and treatment. ACS Chem Neurosci. 2012; 3(11):952-62.
703 45. Xiao Y, Ma B, McElheny D, Parthasarathy S, Long F, Hoshi M, et al. Aβ(1-42)
704 fibril structure illuminates self-recognition and replication of amyloid in
705 Alzheimer’s disease. Nat Struct Mol Biol. 2015; 22(6):499-505.
706 46. Jakki SL, Senthil V, Yasam VR, Chandrasekar MJN, Vijayaraghavan C. The
707 blood brain barrier and its role in Alzheimer’s therapy: an overview. Curr Drug
708 Targets. 2018; 19(2):155-69.
709 47. Jahn H. Memory loss in Alzheimer’s disease. Dialogues Clin Neurosci. 2013;
710 15(4):445-54.
711 48. Kraeuter AK, Guest PC, Sarnyai Z. The Y-maze for assessment of spatial
712 working and reference memory in mice. Methods Mol Biol. 2019; 1916:105-11.
713 49. Lueptow LM. Novel object recognition test for the investigation of learning and
714 memory in mice. J Vis Exp. 2017; (126):55718.
715 50. Qiao O, Ji H, Zhang Y, Zhang X, Zhang X, Liu N, et al. New insights in drug
716 development for Alzheimer’s disease based on microglia function. Biomed
717 Pharmacother. 2021; 140:111703.

718 51. Ahmad MH, Fatima M, Mondal AC. Influence of microglia and astrocyte
719 activation in the neuroinflammatory pathogenesis of Alzheimer's disease:
720 rational insights for the therapeutic approaches. J Clin Neurosci. 2019; 59:6-11.
721 52. Heneka MT, Carson MJ, El Khoury J, Landreth GE, Brosseron F, Feinstein DL,
722 et al. Neuroinflammation in Alzheimer's disease. Lancet Neurol. 2015;
723 14(4):388-405.
724 53. Vekrellis K, Ye Z, Qiu WQ, Walsh D, Hartley D, Chesneau V, et al. Neurons
725 regulate extracellular levels of amyloid β-protein via proteolysis by insulin-
726 degrading enzyme. J Neurosci. 2000; 20(5):1657-65.
727 54. Cook DG, Leverenz JB, McMillan PJ, Kulstad JJ, Ericksen S, Roth RA, et al.
728 Reduced hippocampal insulin-degrading enzyme in late-onset Alzheimer's
729 disease is associated with the apolipoprotein E-ε4 allele. Am J Pathol. 2003;
730 162(1):313-9.
731 55. Eckman EA, Eckman CB. Aβ-degrading enzymes: modulators of Alzheimer's
732 disease pathogenesis and targets for therapeutic intervention. Biochem Soc
733 Trans. 2005; 33(5):1101-5.
734 56. Massaad CA, Klann E. Reactive oxygen species in the regulation of synaptic
735 plasticity and memory. Antioxid Redox Signal. 2011; 14(10):2013-54.
736 57. Kim YS, Gupta Vallur P, Phaëton R, Mythreye K, Hempel N. Insights into the
737 dichotomous regulation of SOD2 in cancer. Antioxidants. 2017; 6(4):86.
738 58. Esposito L, Raber J, Kekonius L, Yan F, Yu GQ, Bien-Ly N, et al. Reduction
739 in mitochondrial superoxide dismutase modulates Alzheimer's disease-like
740 pathology and accelerates the onset of behavioral changes in human amyloid
741 precursor protein transgenic mice. J Neurosci. 2006; 26(19):5167-79.
742 59. Tadokoro K, Ohta Y, Inufusa H, Loon AFN, Abe K. Prevention of cognitive
743 decline in Alzheimer's disease by novel antioxidative supplements. Int J Mol
744 Sci. 2020; 21(6):1974.
745 60. Milkovic L, Cipak Gasparovic A, Cindric M, Mouthuy PA, Zarkovic N. Short
746 overview of ROS as cell function regulators and their implications in therapy
747 concepts. Cells. 2019; 8(8):793.
748 61. Unoki T, Abiko Y, Toyama T, Uehara T, Tsuboi K, Nishida M, et al.
749 Methylmercury, an environmental electrophile capable of activation and
750 disruption of the Akt/CREB/Bcl-2 signal transduction pathway in SH-SY5Y
751 cells. Sci Rep. 2016; 6(1):28944.

752 62. Jin Y, Wang H. Naringenin inhibit the hydrogen peroxide-induced SH-SY5Y
753 cells injury through Nrf2/HO-1 pathway. Neurotox Res. 2019; 36(4):796-805.
754 63. Sun P, Nie X, Chen X, Yin L, Luo J, Sun L, et al. Nrf2 signaling elicits a
755 neuroprotective role against PFOS-mediated oxidative damage and apoptosis.
756 Neurochem Res. 2018; 43(12):2446-59.
757 64. Lepock JR. Protein denaturation during heat shock. Adv Mol Cell Biol. 1997;
758 19:223-59.
759 65. Chaplin V, Caskey CF. Multi-focal HIFU reduces cavitation in mild-
760 hyperthermia. J Ther Ultrasound. 2017; 5(1):12.
761 66. Partanen A, Tillander M, Yarmolenko PS, Wood BJ, Dreher MR, Kohler MO.
762 Reduction of peak acoustic pressure and shaping of heated region by use of
763 multifoci sonications in MR-guided high-intensity focused ultrasound mediated
764 mild hyperthermia. Med Phys. 2013; 40(1):013301.

Figure 1

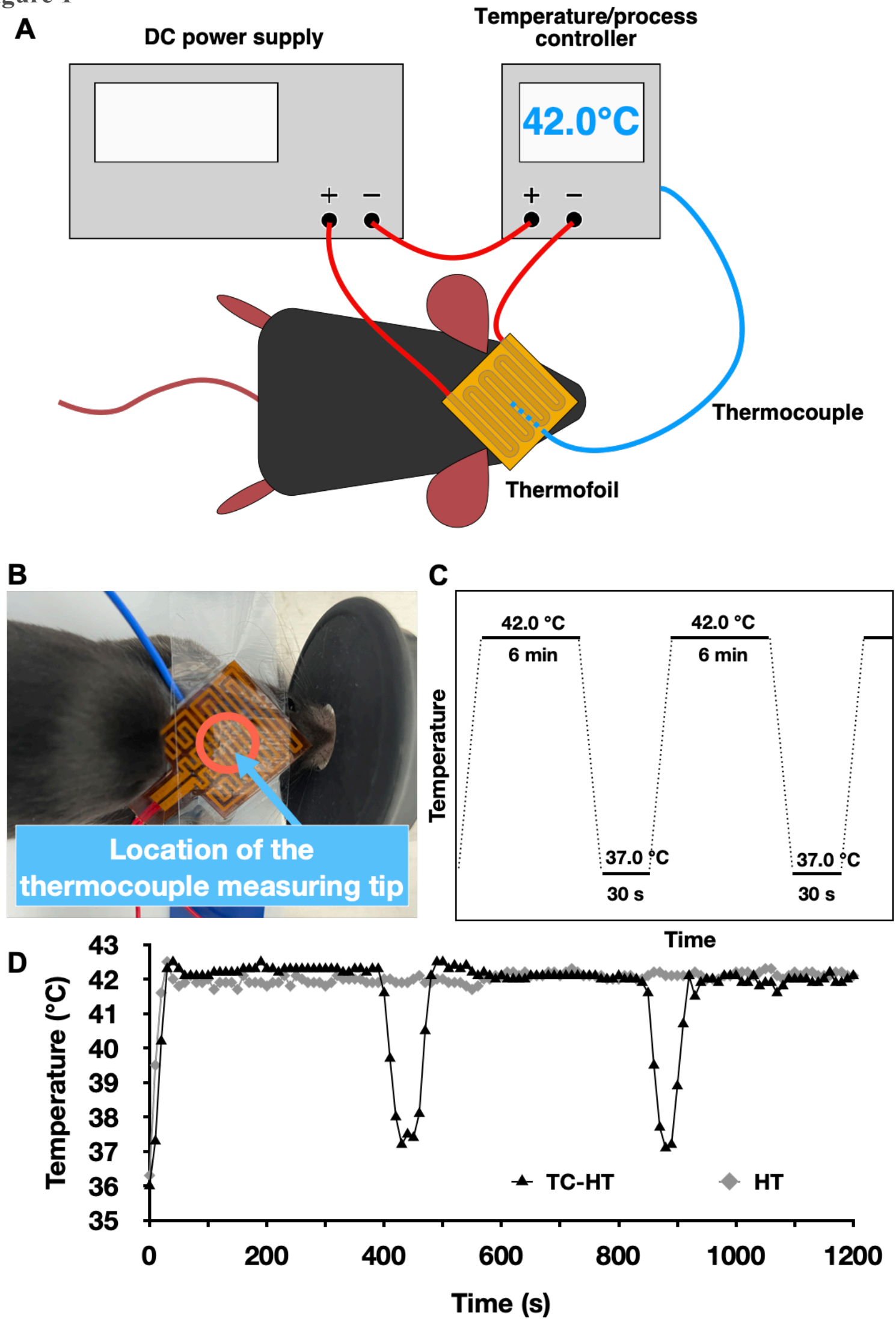
A
DC power supply
Temperature/process controller
42.0°C
+
−
+
−
Thermocouple
Thermofoil
B
Location of the thermocouple measuring tip
C
42.0 °C
6 min
42.0 °C
6 min
37.0 °C
30 s
37.0 °C
30 s
Temperature
Time
D
Temperature (°C)
43
42
41
40
39
38
37
36
35
0
200
400
600
800
1000
1200
Time (s)
TC-HT
HT

Figure 2

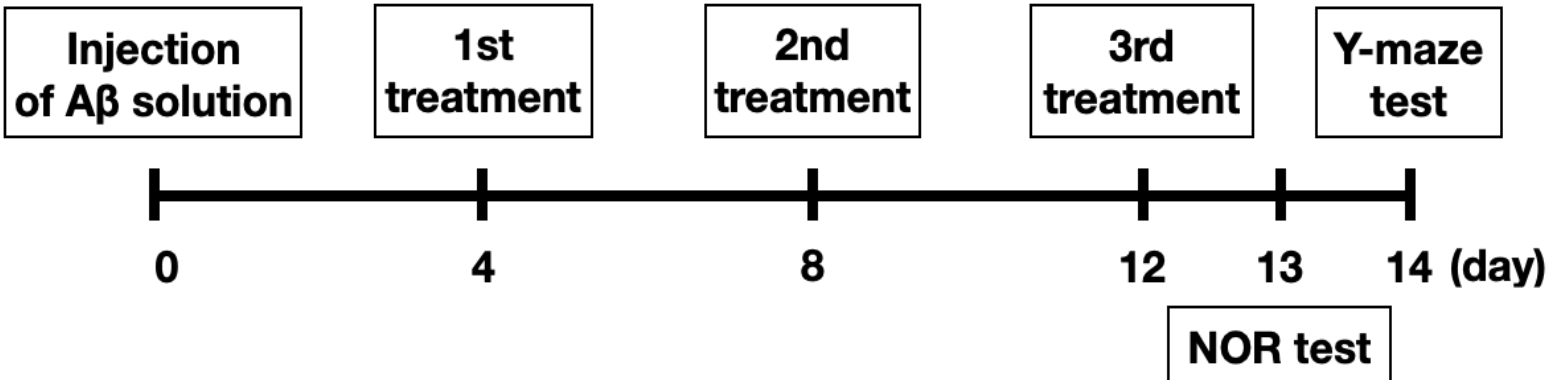
Injection of Aβ solution
1st treatment
2nd treatment
3rd treatment
Y-maze test
0
4
8
12
13
14 (day)
NOR test

Figure 3

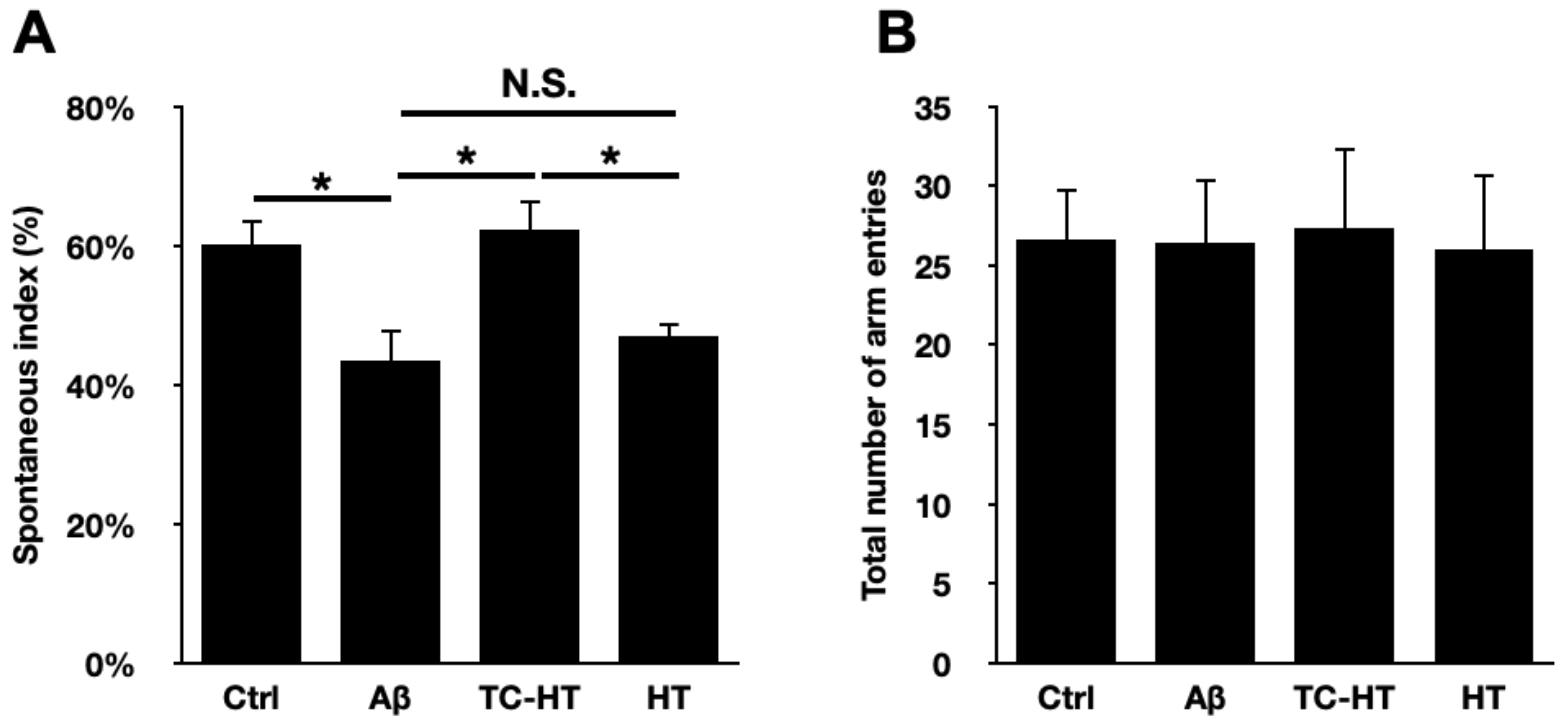
A
N.S.
*
*
*
80%
60%
40%
20%
0%
Spontaneous index (%)
Ctrl
Aβ
TC-HT
HT
B
35
30
25
20
15
10
5
0
Total number of arm entries
Ctrl
Aβ
TC-HT
HT

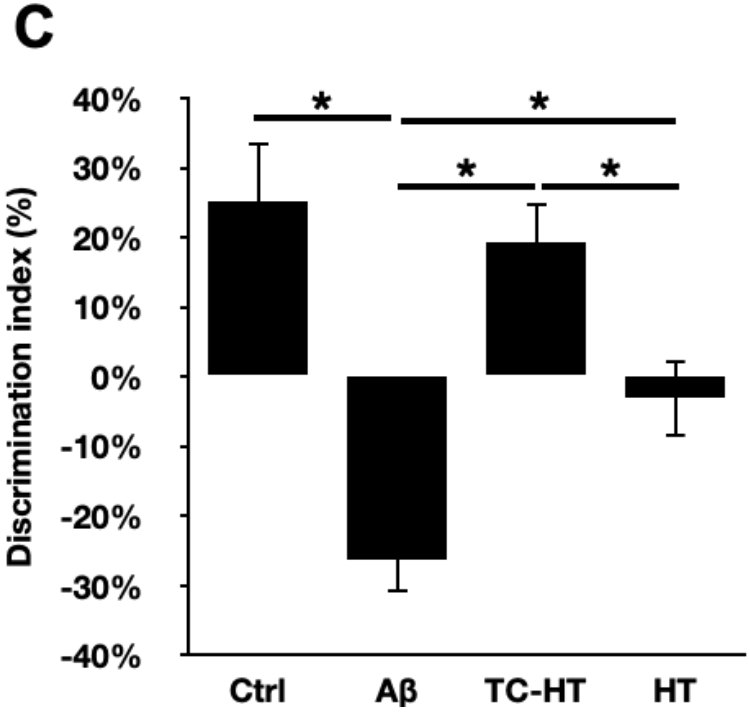
C
*
*
*
*
40%
30%
20%
10%
0%
-10%
-20%
-30%
-40%
Discrimination index (%)
Ctrl
Aβ
TC-HT
HT

Figure 4

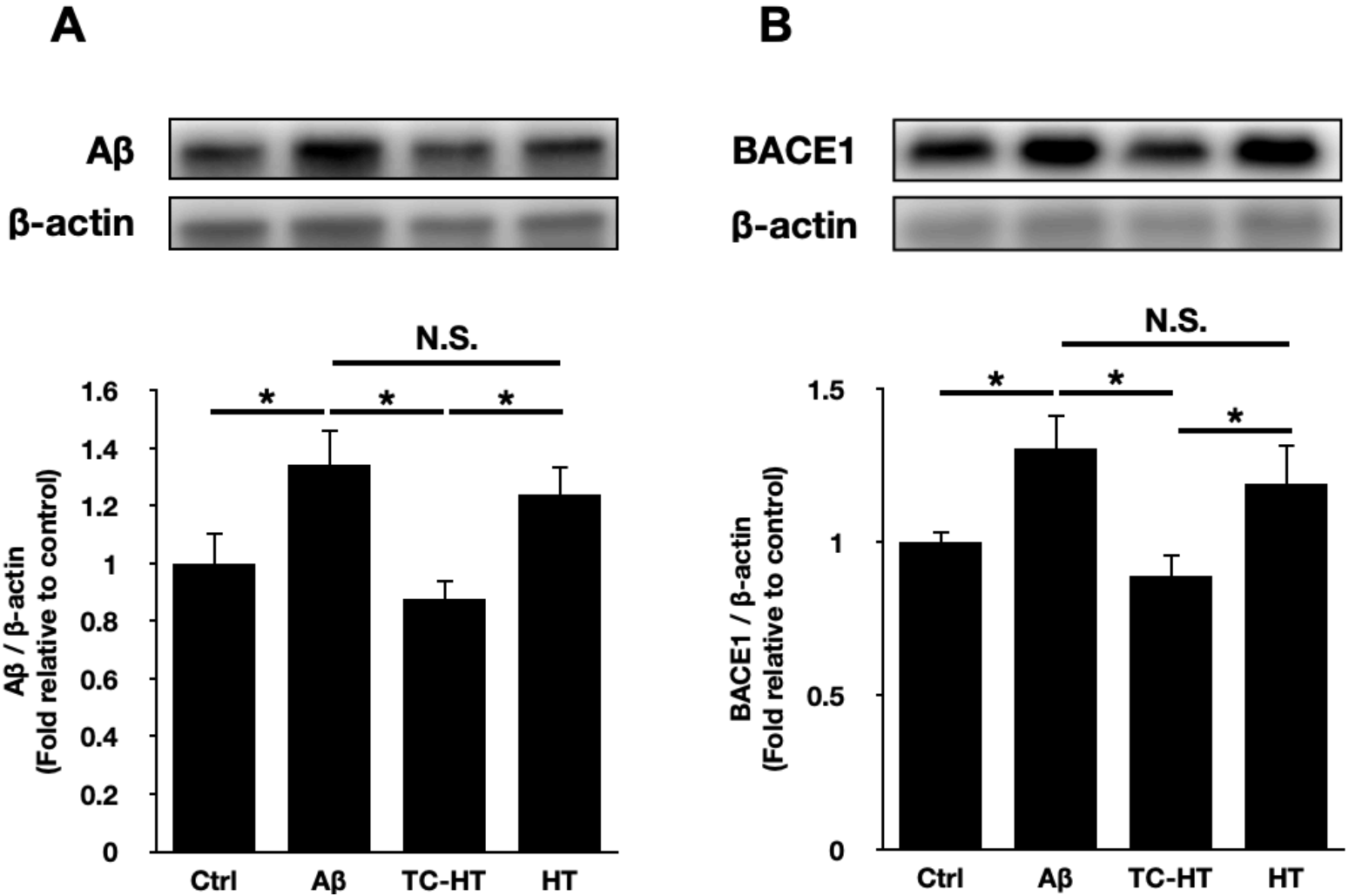
A
Aβ
β-actin
N.S.
*
*
*
1.6
1.4
1.2
1
0.8
0.6
0.4
0.2
0
Aβ / β-actin
(Fold relative to control)
Ctrl
Aβ
TC-HT
HT
B
BACE1
β-actin
N.S.
*
*
*
1.5
1
0.5
0
BACE1 / β-actin
(Fold relative to control)
Ctrl
Aβ
TC-HT
HT

Figure 5

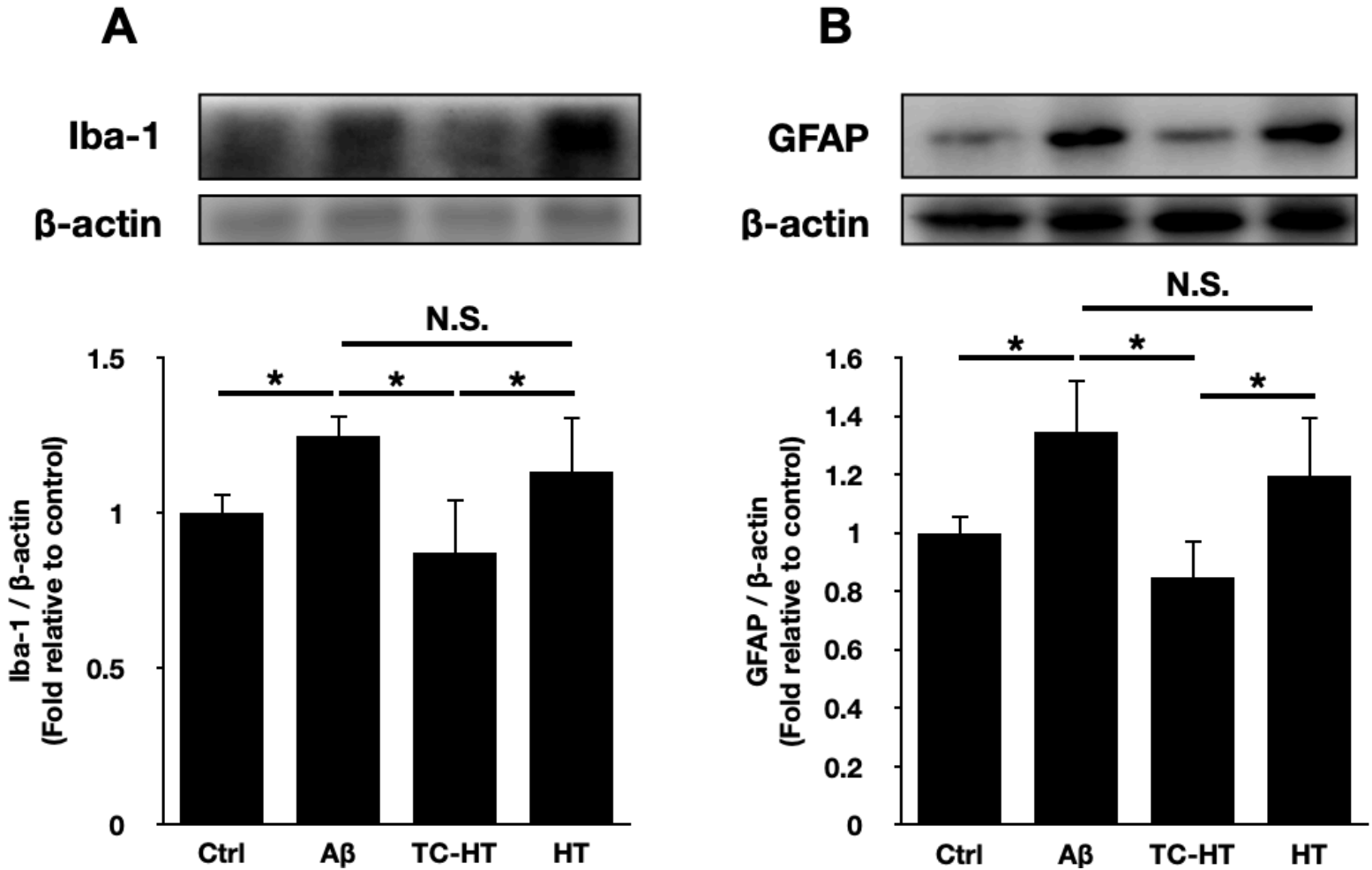
A
Iba-1
β-actin
N.S.
*
*
*
1.5
1
0.5
0
Iba-1 / β-actin
(Fold relative to control)
Ctrl
Aβ
TC-HT
HT
B
GFAP
β-actin
N.S.
*
*
*
1.6
1.4
1.2
1
0.8
0.6
0.4
0.2
0
GFAP / β-actin
(Fold relative to control)
Ctrl
Aβ
TC-HT
HT

Figure 6

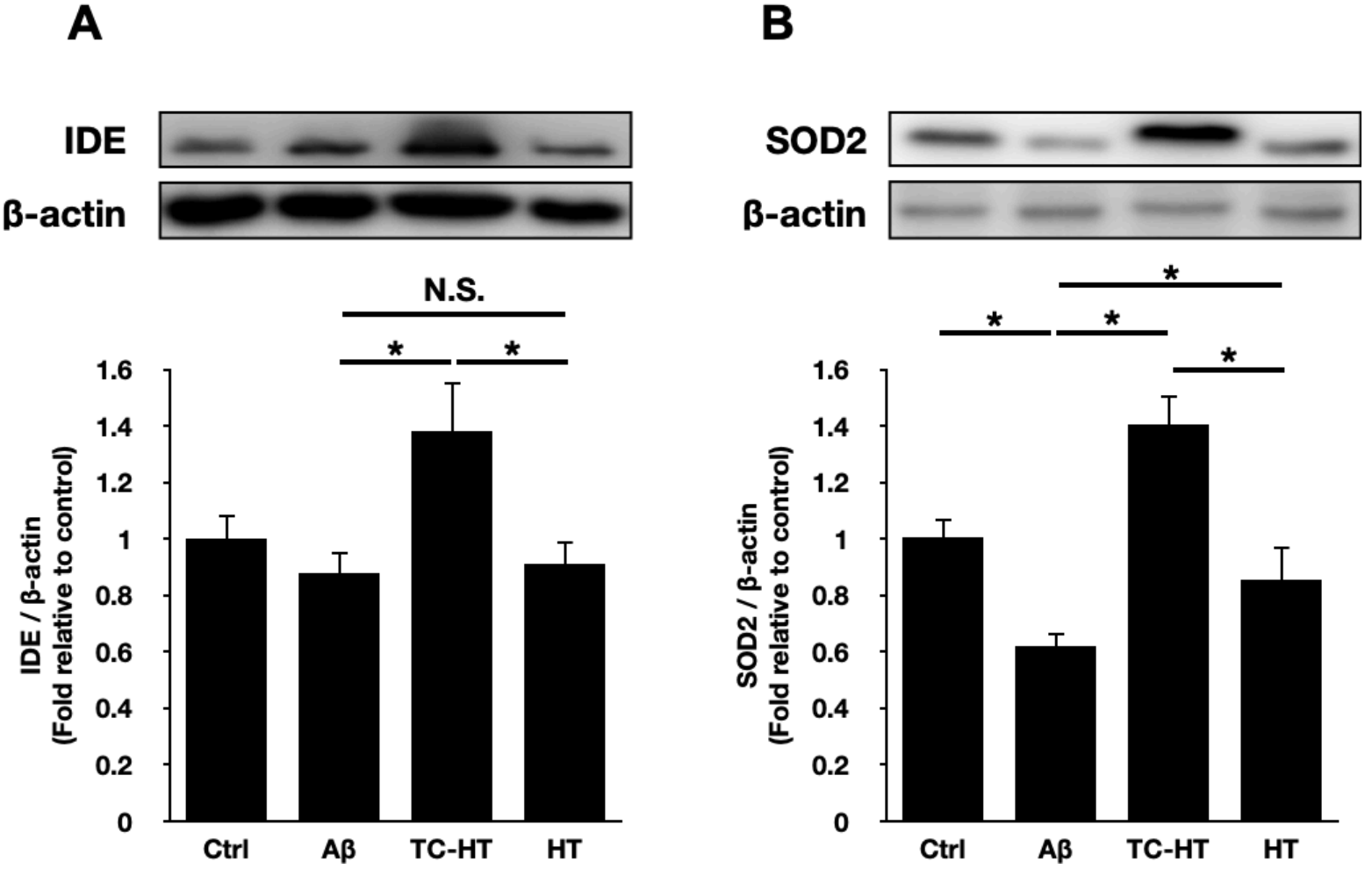
A
IDE
β-actin
N.S.
*
*
IDE / β-actin
(Fold relative to control)
1.6
1.4
1.2
1
0.8
0.6
0.4
0.2
0
Ctrl
Aβ
TC-HT
HT
B
SOD2
β-actin
*
*
*
*
SOD2 / β-actin
(Fold relative to control)
1.6
1.4
1.2
1
0.8
0.6
0.4
0.2
0
Ctrl
Aβ
TC-HT
HT

Figure 7

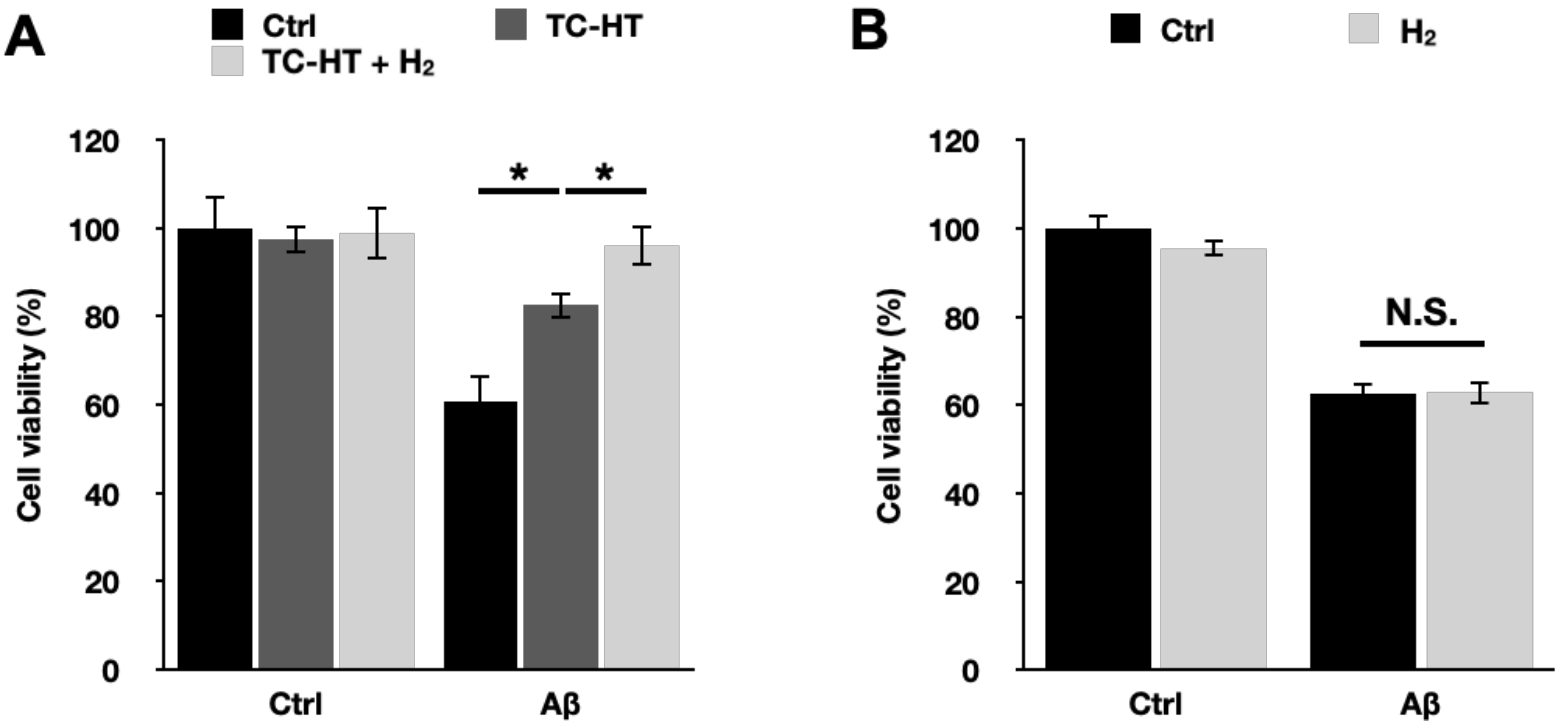
A
Ctrl
TC-HT
TC-HT + H2
Cell viability (%)
120
100
80
60
40
20
0
*
*
Ctrl
Aβ
B
Ctrl
H2
Cell viability (%)
120
100
80
60
40
20
0
N.S.
Ctrl
Aβ